

# Small-angle goniometry for backscattering measurements in the broadband spectrum

Sanna Kaasalainen, Jouni Peltoniemi, Jyri Näränen, Juha Suomalainen, Mikko Kaasalainen, and Folke Stenman

We present experiments on spectral bidirectional reflectance distribution function (BRDF) effects at backscatter and discuss the feasibility of new methods for laboratory and field simulations of remote sensing of land surfaces. The extreme sharpness of the intensity peak allows both directional and comparative experimental spectral studies of hot spots. We demonstrate wavelength-dependent features in the hot-spot reflectance signatures that facilitate extension of spectral and directional BRDF measurements of natural targets (such as forest understories and ice surfaces) into retroreflection to exploit their hot-spot characteristics in the interpretation of spaceborne and airborne data. © 2005 Optical Society of America

*OCIS codes:* 290.1350, 290.5820, 280.0280.

## 1. Introduction

The bidirectional reflectance distribution function (BRDF) describes the directional features of light reflected from a surface (see Fig. 1). These features are characteristic of surface structure and have led to applications in both terrestrial and planetary remote sensing for characterizing targets and retrieving the textural properties of surfaces.<sup>1–3</sup> Laboratory and field data are especially useful in developing methods for investigating spatially complex targets, such as forests and vegetation canopies.

The BRDF at small phase (light source–target–detector) angles is often studied as a special case, both because it requires special instrumentation to prevent the detector from obscuring the light source (see Fig. 1) and because it is utilized in several applications described below. A surge in brightness near zero phase (often referred to as exact backscattering to distinguish it from backward scattering, i.e., reflection to the same hemisphere as the light source)

is a common feature of most remote-sensing targets, such as forest and vegetation,<sup>4,5</sup> where it is seen as a bright spot (called a hot spot) in satelliteborne or airborne images. The BRDFs for field targets (such as lichen<sup>6,7</sup>), measured with ground-based goniometers, often show enhancement in the backward direction, although zero phase has not been reached. This phenomenon is known in planetary science as the opposition effect and has been studied for decades for solar system regolith surfaces and ices (e.g., Saturn's rings).<sup>8–10</sup> In condensed-matter physics, narrow coherent backscattering peaks are observed on a milliradian scale. The effect is called weak localization (of photons), and it has been the subject of various studies, mostly of small particles.<sup>11,12</sup> Applications include medicine, in which backscattering instruments facilitate use of noncontact diagnostic methods.<sup>13</sup> Radar backscattering signatures from land surfaces have also been shown to be distinguishable such that they can be utilized in radar scatterometers for, e.g., identification of snow-free and snow-covered areas.<sup>14</sup> Backscattering is involved in laser scanning altimetry,<sup>15</sup> but the intensity data have not been used thus far. Some complicated physical mechanisms also make BRDF near backscattering a special case: The current physical phenomena related to brightening are shadow hiding and coherent backscattering, but their contributions to the intensity peak are somewhat difficult to separate in experimental data.<sup>4,16</sup> Changes in the polarization ratio are also common near backscatter, and the polarization features seem to be even more distinctive than intensity effects.

---

S. Kaasalainen (sanna.kaasalainen@fgi.fi), J. Peltoniemi, J. Näränen, and J. Suomalainen are with the Finnish Geodetic Institute, Geodeetinrinne 2 (P.O. Box 15), FIN-02431 Masala, Finland. M. Kaasalainen is with the Department of Mathematics and Statistics, P.O. Box 68, FIN-00014 University of Helsinki, Finland. F. Stenman is with the Department of Physical Sciences, P.O. Box 64, FIN-00014 University of Helsinki, Finland.

Received 25 June 2004; revised manuscript received 19 October 2004; accepted 4 November 2004.

0003-6935/05/081485-06\$15.00/0

© 2005 Optical Society of America

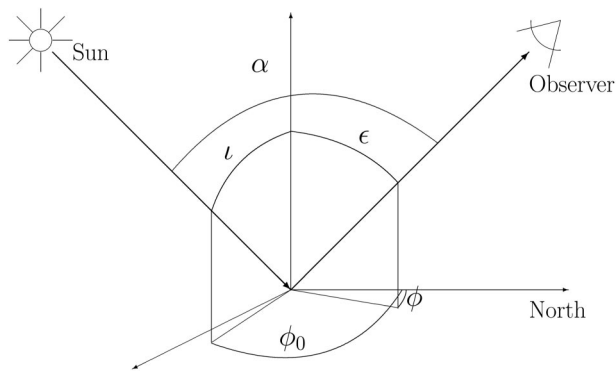


Fig. 1. Geometry of BRDF measurement:  $\epsilon$  and  $\iota$  are angles of emergence and incidence, respectively. The principal plane is defined by Sun, target, and Observer, and  $\alpha$  is the phase angle between them. ( $\phi$  and  $\phi_0$  are the corresponding azimuths for emergence and incidence.) At  $\alpha = 0^\circ$  the detector obscures the light source. The small-angle goniometer discussed in this paper is utilized to include zero phase in the study.

Thus far, polarization has received more attention in studies of optics and biological media,<sup>17</sup> but it has found a few applications in planetary and space studies as well.<sup>10,16</sup>

Few laboratory measurements have been available for reference in the study of land surfaces, except in a few special cases designed for studying the physical mechanisms that cause hot spots and the opposition effect of ices.<sup>18</sup> No comparisons of ground measurements with data from remote-sensing instruments that observe in retroreflection (such as POLDER: polarization and directionality of the Earth's reflectances<sup>5</sup>) have been available for systematic study. Backscattering enhancement has been studied in the laboratory mostly by use of lasers and diodes<sup>19</sup> because their collimated beams permit easy alignment, but no spectral information has been reported. The method has been applied mostly for small-scale samples, such as powdered minerals and chemicals.<sup>10,20,21</sup> Laser- and diode-based devices are also widely used in optics and medicine for interferometric purposes.<sup>13,17,22</sup>

The dependence of backscattering on wavelength has been observed for planetary targets. There are variations of as much as 10% in magnitude, such as the reddening of the asteroid 433 Eros with increasing phase angle<sup>23</sup> and variations in brightness of Saturn's rings between 0.555 and 0.336  $\mu\text{m}$  at  $>1^\circ$  phase angles.<sup>8</sup> There are practically no broadband or spectroscopic small-angle experiments for ground reference. One of the few laboratory studies thus far produced no difference between results at 0.543 and 0.633  $\mu\text{m}$  for aluminum oxide.<sup>24</sup>

The importance of hot-spot signatures for airborne and satelliteborne remote sensing has been pointed out for measuring leaf reflectances and canopy structures.<sup>5</sup> The systematic exploitation of hot spots in surface characterization is still in its infancy, and the use of hot spots in the interpretation of remote data (from both terrestrial and planetary objects) still

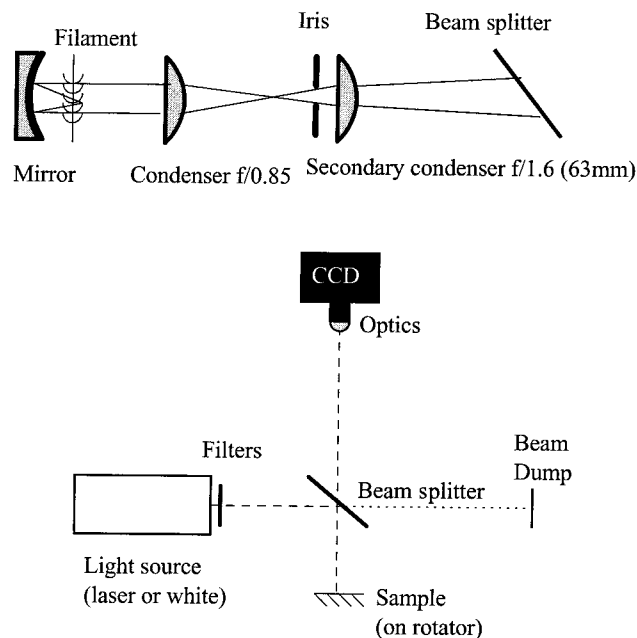


Fig. 2. Illustration of the QTH lamp system (top) and the experimental setup (bottom). The distances from the lamp and the laser to the beam splitter were 13 and 100 cm, respectively (having the QTH source closer than the laser to the beam splitter was crucial for the alignment), 7–10 cm from the beam splitter to the sample (depending on what sample is used), and 125 cm from the CCD lens to the sample. The QTH and laser spot diameters on the sample were 2.5 cm and 2–3 mm, respectively.

needs to be assessed with extensive laboratory measurements and modeling. The fact that different backscattering patterns are applied in many other fields (as discussed above) makes the intensity and polarization effects worth more-comprehensive investigation in land surface studies as well. Controlled laboratory data are essential for the physical study of backscattering.

We have investigated methods of spectral study in backscattering with different setups and extended the laser-based measurement technique to include broadband sources to supply ground references for hot-spot signatures measured by airborne and spaceborne instruments. This is to our knowledge the first (although preliminary) implementation of small-angle spectroscopy for natural targets. The methods are outlined in Section 2. Results and conclusions, with a discussion of suggestions for future improvements, are presented in Sections 3 and 4, respectively.

## 2. Experiment

The instrument was based on a setup used earlier for laser measurements.<sup>20</sup> The backscattering geometry was worked out with a plate beam splitter (see Fig. 2): The reflected spot was retroreflected from the sample and transmitted through the beam splitter into the CCD detector. We achieved nonzero phase angles by rotating the beam splitter to change the angle of incidence upon the sample. The phase angle range was

$-3^\circ$  to  $19^\circ$ ; pluses and minuses refer to the viewing geometry where the spot moved toward and away from the light source, respectively. We rotated the sample to get a larger part of the surface illuminated during the (3-s) exposure and to reduce laser speckle. Neutral-density filters were used in front of the light source to keep the signal in the linear range of the CCD.

Two types of light source were utilized: Lasers and a quartz tungsten halogen (QTH) lamp. The laser wavelengths were 633.2 nm (helium–neon) and 1064 nm (diode-pumped Nd:YAG). For a broadband source we used a QTH lamp with an effective wavelength range from 350 to 2400 nm mounted in an Oriel research housing. We obtained a spot by using a parabolic mirror, an iris, and condensing lenses (Fig. 2). Spot sizes and uniform illumination are limited by filament size. Both visible and near-infrared band beam splitters were used, the former with a He–Ne laser and a QTH lamp and the latter with the infrared laser. We found that the visible beam splitter reflectance–transmittance ratio varies slightly with wavelength, but the deviations in the spectrum can be compensated for by calibration with a spectroscopic standard (Spectralon plate).

We computed the nominal angular resolution of the instrument by summing the angles subtended by source and detector apertures, as seen from the sample. The upper limits of the resolutions for the laser and QTH systems were  $0.4^\circ$ , and  $0.9^\circ$ , respectively. The resolution of the QTH lamp, however, was also affected by reduced accuracy in collimation and alignment, approximated (from the results) to be  $1.5^\circ$ . In practice the resolution levels are from  $0.4^\circ$  to  $0.9^\circ$ , as discussed in Section 3 below.

The spectra were measured with an ASD FieldSpec Pro spectrometer, which had a  $1^\circ$  fore field-of-view optics at the end of an optical fiber, which was placed above the beam splitter. The principal plane BRDFs were measured with the spectrometer mounted in a field goniometer designed for large-angle BRDF spectroscopy<sup>7</sup> and a high-power QTH source.

### 3. Results and Discussion

We present results for aluminum oxide abrasive powder (Micro Abrasives Corporation) of  $1\text{-}\mu\text{m}$  grain size, known to show a sharp backscattering peak [at 632.8 nm (Refs. 10 and 20)]; lichen [*Cladina arbuscula* (Fig. 3)] to demonstrate a natural target with complicated surface structure and a strong signal in the infrared; and a sand sample with a  $125\text{--}250\text{-}\mu\text{m}$  grain size range, sieved from a larger sample taken from Kalajoki dunes, a typical Finnish land target. The samples were chosen because of their different optical properties and suitability for test measurements.

#### A. Brightness Effects

All intensities are presented relative to the intensity of a Spectralon standard (i.e., divided by its average value in the linear part of the phase curve, where its phase curve is close to constant). The reflectances are



Fig. 3. Lichen (*Cladina arbuscula*) sample. The stand was  $\sim 5$  cm high.

plotted in Figs. 4 and 5. The hot-spot signals are prominent for aluminum oxide and lichen, regardless of the light source (although the intensities near zero are rounded in the QTH measurements). A peak also occurs in the laser phase curves of the sand sample. Differences in the signals among samples can be distinguished from all the measurements.

Phase curves of aluminum oxide with all three light sources are compared in Fig. 4 (left). The shape of the phase curve at 1064 nm agrees with the QTH curve down to  $0.7^\circ$ , where the rounding of the QTH measurement takes effect. A slight decrease in intensity at phase angles of  $<5^\circ$  is observed at 1064 nm and with white light but not at 633 nm, which sug-

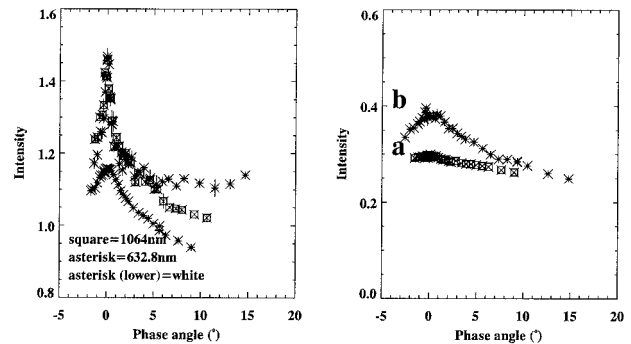


Fig. 4. Left, backscattering peaks for aluminum oxide at 1064 and 632.8 nm and white light (QTH) and right, QTH phase curves of lichen (asterisks) and sand (squares).

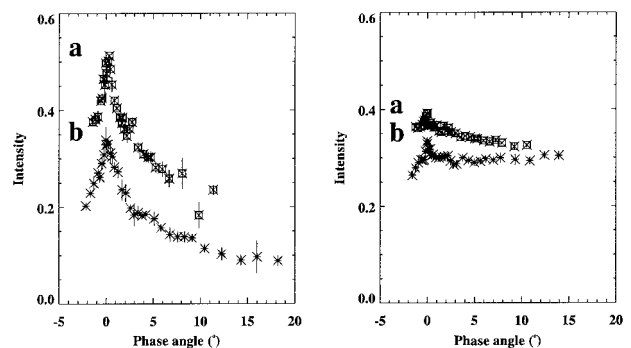


Fig. 5. Comparison of backscattering peaks for lichen (left) and Kalajoki sand (right) measured with a laser at a, 1064 and b, 632.8 nm.

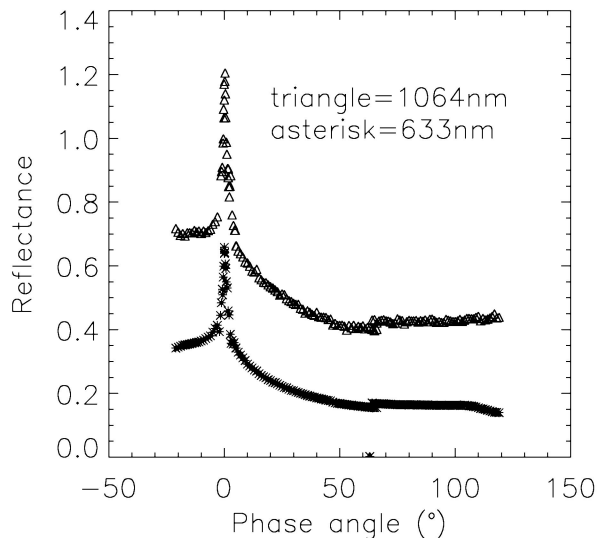


Fig. 6. Comparison of phase curves of the lichen sample at 1064 and 633 nm measured with lasers (from  $-2^\circ$  to  $+5^\circ$ ) and with the spectrogoniometer (other angles).

gests strong wavelength effects with increasing phase angle. The sand sample shows a similar effect [differences at larger phase angles have also been observed for, e.g. asteroid 433 Eros (Ref. 23)], but for lichen the intensities seem to drop for all measured examples.

To give an example of extended BRDF spectrogoniometry and illustrate the magnitude of the backscattering surge over a large-angle scale, we combined the laser phase curves for lichen with the principal plane measurements (see Fig. 1 for the geometry) at 1064 and 633 nm (Fig. 6). We made the plots by normalizing the laser intensities with the principal plane BRDF at  $5^\circ$ . More research needs to be done for better compatibility (the intensity levels do not coincide because of, e.g., polarization and different angles of incidence).

### B. Spectral Effects

The amplitudes of the brightness surges [ $I(0^\circ)/I(5^\circ)$ ] are compared in Table 1. The lichen sample shows a striking difference between the magnitudes of the surge at 1064 and 632.8 nm, whereas for aluminum oxide ( $\text{Al}_2\text{O}_3$ ) the difference is within the measurement error. This is also seen in the corresponding plots in Figs. 4 and 5. Nelson *et al.*<sup>24</sup> found no difference for aluminum oxide at 633 and at 543 nm. Com-

Table 1. Comparison of Backscattering Peak Amplitudes<sup>a</sup>

Sample	Laser Intensity		
	1064 (nm)	632.8 (nm)	White Light (nm)
$\text{Al}_2\text{O}_3$	1.33	1.31	1.15
Sand	1.15	1.13	1.07
Lichen	1.69	1.87	1.17

<sup>a</sup>Measured here as  $I(0^\circ)/I(5^\circ)$ , where  $I$  is the intensity.

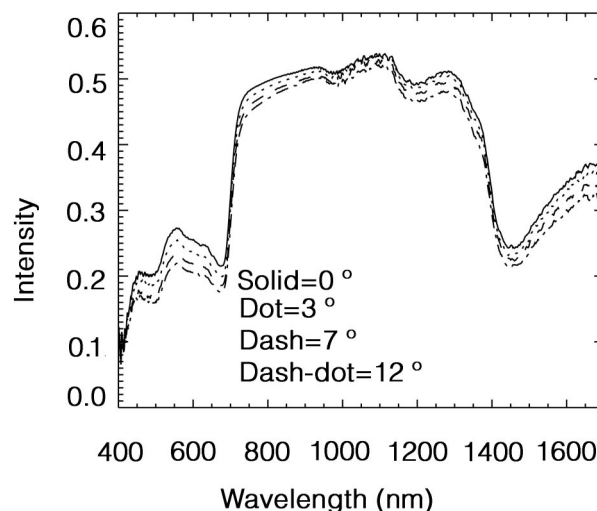


Fig. 7. Spectra of lichen at increasing phase angles. The variations in intensity from  $0^\circ$  to  $12^\circ$  are of the order of 3% at 1064 nm, 20% at 633 nm, and 15% at 1500 nm.

bined with the present result, this implies that for more than a factor of 2 in wavelength there appears to be no dependence on wavelength of the angular width of the brightness surge, which is difficult to explain by use of the coherent backscatter models that predict a strong wavelength dependence.<sup>24</sup> The QTH peaks are smaller because of rounding, but the differences between samples are in qualitative agreement with those from laser data.

To get insight into the wavelength effects in the broadband spectrum we made an exploratory plot of spectra at approximately  $0^\circ$ ,  $3^\circ$ ,  $7^\circ$ , and  $12^\circ$  phase angles (Fig. 7). Although the limited accuracy of this experiment has smoothed out the effects, clear differences can be observed in the spectrum as the phase angle increases. The variations are strongest near 600 and 1500 nm. Stronger variation at 600 nm than at 1064 nm was also shown with lasers (Table 1).

### C. Effect of Instrument Resolution

The angular resolution of the instrument is crucial because of the extremely spiked nature of the brightness surge near  $0^\circ$ . Better resolution is obtained with lasers, but no such collimation can be achieved with a white-light source, such as the QTH lamp used in the present study or the broadband sources used in most BRDF goniospectrometers. We investigated the rounding of the phase curve, using a simple realistic form for intensity  $I$  as a function of phase angle  $x$ :

$$I(x) = c \exp(-|x|) + k|x| + d, \quad (1)$$

where  $c$ ,  $k$ , and  $d$  are constants. This is an empirical representation for  $I(x)$  for many surfaces.<sup>18,20</sup> The effect of the resolution width, designated  $a$  here, can be approximately simulated with integration over a slit of width  $a$  at each phase angle  $x$  (at the center of the slit) to get the rounded function  $I_R(x)$ :

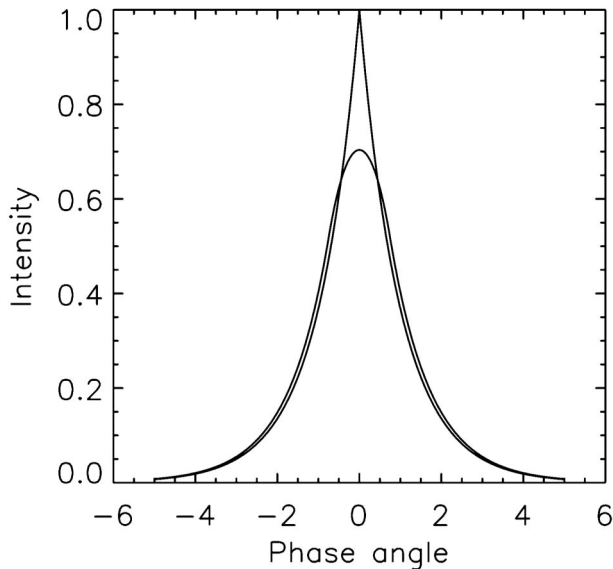


Fig. 8. Rounding of the phase curve with  $1.5^\circ$  angular resolution. The phase curve is illustrated by an exponential function [sharp curve; see Eqs. (1) and (2)].

$$I_R(x) = c \left[ \frac{2 \sinh a/2}{a} \right] \exp(-|x|) + k|x| + d, \quad |x| > \frac{a}{2},$$

$$I_R(x) = c \frac{2}{a} \left( 1 - \exp \frac{-a}{2} \cosh x \right) + \frac{kx^2}{a} + \frac{ka}{4} + d, \quad -\frac{a}{2} < x < \frac{a}{2}. \quad (2)$$

When  $a = 1.5^\circ$  is chosen, as in the case of our QTH source, rounding of the phase curve occurs at phase angles  $-0.75^\circ < x < 0.75^\circ$ , as is demonstrated in Fig. 8 (we chose  $c = 1$  and  $d = 0$  for the plot). The phase curve near  $0^\circ$  is not, however, completely flattened (probably because the peak itself is so sharp) and to some extent represents a sharp effect, and it is possible either to observe the relative differences between surfaces or retrieve more-accurate peak information by deconvolution (although the feasibility of that approach should be further studied). It is also worth noting that the phase curves practically coincide down to  $x = 0.75^\circ$ , which is way below the phase angle range of most goniometers.

#### 4. Conclusions

We studied the methods of broadband and spectral backscattering measurement and investigated their ability to bring out the characteristic optical properties of various samples. We demonstrated an extension of bidirectional reflectance distribution function measurements into a hot-spot region and introduced an experiment for devising backscattering measurements in white light for the directional and comparative spectroscopic study of hot spots. It turned out

that small-angle spectroscopy is a source of further information and can be used as a characterization tool, especially for natural targets. In the absence of high collimation small-angle spectrogoniometers, the application of a particular instrument is critically dependent on its angular resolution:

1. Measuring accurately the properties of a hot spot near  $0^\circ$  phase requires microalignment because of the extremely peaked nature of the brightness surge. For a quantitative physical study of and information on peak properties, a coherent light source is needed, although the utmost—almost superexponential—sharpness of the surge sets a limit for its well-defined observation at zero in other than a relative sense. Lasers have proved superior in directional and wavelength case studies but are limited to narrow-wavelength bands.

2. Differences in peak properties are observable, at least qualitatively, with noncoherent (broadband) sources as well. The broadband light source is capable of facilitating a relative study of spectral effects in backscattering and of providing a reference for remote observations. There is a demand for this information because many remote-sensing instruments observe hot spots. Inasmuch as they are the only means of small-angle BRDF spectroscopy thus far, broadband sources are worth further development for better collimation and accuracy. For remote instruments that use the Sun as a light source, the size of the solar disk fixes the smallest angular resolution to  $0.5^\circ$ .

There are several extensions for the methods presented here. The use of larger (than laser) spot sizes will facilitate the study of scale effects in backscatter, which play a role in the comparison of data from various instruments. A combination of multiangular (BRDF) and backscatter data would also enhance the empirical testing of light-scattering models on an extended angular scale. Deconvolution of data near  $0^\circ$  holds the prospect of extrapolation of measurements (cf. Ref. 17), at least to provide phenomenological insight into the peak properties closer to  $0^\circ$  than any instrument permits.

We are working toward further development of a small-angle goniometer for improved resolution, alignment, positioning, and more-accurate albedo measurement. The problems to be addressed in the future include finding the most suitable wavelength and angular ranges for signature studies and use of the versatility of the present instrument to simulate adequately the various remote-sensing experiments in the laboratory.

We extend many thanks to Kalle Palomäki of Helsinki University of Technology for supplying an abundance of sand samples and Miina Rautiainen of the University of Helsinki for information on lichen. We also thank an anonymous referee for a review that led to material improvements. This research was sup-

ported by The Finnish Society of Sciences and Letters and the Academy of Finland.

## References

1. J.-L. Widlowski, B. Pinty, N. Gobron, and M. Verstraete, "Detection and characterization of boreal coniferous forests from remote sensing data," *J. Geophys. Res.* **106**, 405–419 (2001).
2. J.-G. Winther, S. Gerland, J. B. Ørbæk, B. Ivanov, A. Blanco, and J. Boike, "Spectral reflectance of melting snow in a high Arctic watershed on Svalbard: some implications for optical remote sensing studies," *Hydrol. Process.* **13**, 2033–2039 (1999).
3. G. P. Asner and A. S. Warner, "Canopy shadow in IKONOS satellite observations of tropical forests and savannas," *Remote Sens. Environ.* **87**, 521–533 (2003).
4. B. Hapke, D. DiMucci, R. Nelson, and W. Smythe, "The cause of the hot spot in vegetation canopies and soils: shadow-hiding versus coherent backscatter," *Remote Sens. Environ.* **58**, 63–68 (1995).
5. F. Camacho-de-Coca, F. M. Brèon, M. Leroy, and F. J. Garcia-Haro, "Airborne measurement of hot spot reflectance signatures," *Remote Sens. Environ.* **90**, 63–75 (2004).
6. I. Solheim, O. Engelsen, B. Hosgood, and G. Andreoli, "Measurement and modeling of the spectral and directional reflection properties of lichen and moss canopies," *Remote Sens. Environ.* **72**, 78–94 (2000).
7. J. Peltoniemi, S. Kaasalainen, J. Näränen, M. Rautiainen, P. Stenberg, H. Smolander, S. Smolander, and P. Voipio, "BRDF measurement of understory vegetation in pine forests: dwarf shrubs, lichen and moss," *Remote Sens. Environ.* (to be published).
8. F. Poulet, J. N. Cuzzi, R. G. French, and L. Dones, "A study of Saturn's ring phase curves from HST observations," *Icarus* **158**, 224–248 (2002).
9. I. Belskaya and V. Shevchenko, "Opposition effect of asteroids," *Icarus* **147**, 94–105 (2000).
10. R. M. Nelson, B. W. Hapke, W. D. Smythe, and L. J. Spilker, "The opposition effect in simulated planetary regoliths. Reflectance and circular polarization ratio change at small phase angle," *Icarus* **147**, 545–558 (2000).
11. Y. Kuga and A. Ishimaru, "Retroreflectance from a dense distribution of spherical particles," *J. Opt. Soc. Am. A* **1**, 831–835 (1984).
12. D. S. Wiersma, M. P. van Albada, B. A. van Tiggelen, and A. Lagendijk, "Experimental evidence for recurrent multiple scattering events of light in disordered media," *Phys. Rev. Lett.* **74**, 4193–4196 (1995).
13. M. Wojtkowski, T. Bajraszewski, P. Targowski, and A. Kowalczyk, "Real-time *in vivo* imaging by high-speed spectral optical coherence tomography," *Opt. Lett.* **28**, 1745–1747 (2003).
14. T. Strozzi and C. Mätzler, "Backscattering measurements of Alpine snowcovers at 5.3 and 35 GHz," *IEEE Trans. Geosci. Remote Sens.* **36**, 838–848 (1998).
15. K. Kraus and N. Pfeifer, "Determination of terrain models in wooded areas with airborne laser scanner data," *ISPRS J. Photogramm. and Remote Sens.* **53**, 193–203 (1998).
16. Yu. Shkuratov, A. Ovcharenko, E. Zubko, O. Miloslavskaya, K. Muinonen, J. Piironen, R. Nelson, W. Smythe, V. Rosenbush, and P. Helfenstein, "The opposition effect and negative polarization of structural analogs for planetary regoliths," *Icarus* **159**, 396–416 (2002).
17. G. Yoon, D. N. G. Roy, and R. C. Straight, "Coherent backscattering in biological media: measurement and estimation of optical properties," *Appl. Opt.* **32**, 580–585 (1993).
18. J. Piironen, K. Muinonen, S. Keränen, H. Karttunen, and J. I. Peltoniemi, "Backscattering of light by snow: field measurements," in *Observing Land from Space: Science, Customers, and Technology*, M. M. Verstraete, M. Meneti, and J. Peltoniemi, eds. (Kluwer, Dordrecht, The Netherlands, 2000), pp. 219–228.
19. S. Kaasalainen, J. Piironen, K. Muinonen, H. Karttunen, and J. Peltoniemi, "Laboratory experiments on backscattering from regolith samples," *Appl. Opt.* **41**, 4416–4420 (2002).
20. S. Kaasalainen, "Laboratory photometry of planetary regolith analogs. I. Effects of grain and packing properties of the opposition effect," *Astron. Astrophys.* **409**, 765–769 (2003).
21. J. Näränen, S. Kaasalainen, J. Peltoniemi, S. Heikkilä, M. Granvik, and V. Saarinen, "Laboratory photometry of planetary regolith analogs. II. Surface roughness and extremes of packing density," *Astron. Astrophys.* **426**, 1103–1109 (2004).
22. M. Wax, C. Yang, R. R. Dasari, and M. S. Feld, "Measurement of angular distributions by use of low-coherence interferometry for light-scattering spectroscopy," *Opt. Lett.* **26**, 322–324 (2001).
23. B. E. Clark, P. Helfenstein, J. F. Bell III, C. Peterson, J. Veverka, N. I. Izenberg, D. Wellnitz, and L. McFaden, "Near infrared spectrometer photometry of asteroid 433 Eros," *Icarus* **155**, 189–204 (2002).
24. R. M. Nelson, W. D. Smythe, B. W. Hapke, and A. S. Hale, "Low phase angle laboratory studies of the opposition effect: search for wavelength dependence," *Planet. Space Sci.* **50**, 849–856 (2002).